Pediatr Radiol (2005) 35: 3–10
DOI 10.1007/s00247-004-1219-3

MINISYMPOSIUM

Taylor Chung

Magnetic resonance angiography of the body in pediatric patients: experience with a contrast-enhanced time-resolved technique

Received: 31 December 2003
Revised: 15 March 2004
Accepted: 7 April 2004
Published online: 22 June 2004

T. Chung
Edward B Singleton Department of Diagnostic Imaging, Texas Children's Hospital, 6621 Fannin Street, MC 2-2521, Houston, TX 77030, USA
E-mail: txchung@texaschildrenshospital.org
Tel.: +1-832-8245324
Fax: +1-832-8255241

T. Chung
Department of Radiology, Baylor College of Medicine, Houston, TX, USA

Abstract This paper reviews the general technique of contrast-enhanced magnetic resonance angiography (CE-MRA) and the challenges of applying CE-MRA to pediatric patients. In particular, the application of "time-resolved" CE-MRA on a commercially available MR scanner using parallel imaging technique such as sensitivity encoding (SENSE) is discussed in detail. Multiple clinical case examples are provided to highlight the broad clinical application of this particular technique and the ease of use of this technique. The main limitation of this technique is dictated by the trade-off between temporal and spatial resolution. Finally, some potential future techniques that may be able to provide better MRA in freely breathing pediatric patients are suggested.

Keywords Magnetic resonance · Magnetic resonance angiography

Introduction

There are numerous magnetic resonance (MR) techniques currently available to perform cardiovascular angiography. Since Prince et al. [1] in 1993 first reported the clinical use of contrast-enhanced MR angiography (CE-MRA) for adult abdominal aortography, CE-MRA has been the technique of choice for body MRA in the adult population. Because of the long breath-hold period required by the early implementations of CE-MRA, this technique was initially not suitable for the pediatric population. However, as scan times became shorter, many different groups found various clinical applications for CE-MRA in the pediatric population and various techniques were utilized [2–13]. As the technique further evolved with the rapid advancement of MR hardware, including stronger and faster gradients, and MR pulse sequence design, including more clever and efficient k-space trajectories [14–18] coupled with parallel imaging techniques [19–21], the scan time has significantly decreased. A detailed explanation of parallel imaging [19–21] is beyond the scope of this paper, but briefly, parallel imaging can be theoretically thought of as imaging different parts of the field-of-view (FOV) simultaneously, thereby shortening the acquisition time. A multi-element phased-array coil is required. Each element of the coil actually receives signal from the entire imaging volume, and therefore there is redundant information in the signal received by the phased-array coil from the imaging volume. Thus, one can cleverly exploit this redundancy of data and shorten the acquisition time. In SENSE or sensitivity encoding [20], which is one type of parallel imaging technique, this "exploitation" is made in the image space domain. In another implementation of parallel imaging, SMASH or simultaneous acquisition of spatial harmonics [19], the exploitation is made in the k-space domain. By taking advantage of this decrease in scan time provided by

parallel imaging techniques, one simple implementation of "time-resolved" CE-MRA that has been used in the pediatric population is described here.

General technique of CE-MRA

The T1 of blood can be significantly shortened by the presence of gadolinium contrast agent. Therefore, by using a T1-weighted sequence, the blood in the vessel will have high signal intensity. To achieve high spatial resolution and minimize scan time, a 3D T1-weighted fast gradient echo sequence is implemented. Since the center of k-space controls the contrast of the corresponding image, the bolus of gadolinium contrast agent needs to arrive at the vessel of interest when the 3D T1-weighted fast-gradient echo sequence is acquiring data for the center of k-space. Therefore, some form of timing the arrival of the contrast bolus to the vessel of interest is needed. This is either done by a best estimate or a timing scan with a small test bolus of contrast prior to the actual CE-MRA, or by some automated method of tracking the actual contrast bolus and triggering the start of the CE-MRA sequence [15]. Coupled with contrast bolus timing is some type of k-space filling scheme or k-space trajectory such that the center of k-space is filled with the initial echoes of the CE-MRA sequence. This is typically known as centric k-space trajectory [14, 16, 18]. Finally, to achieve the best quality MRA, breath-holding is needed to avoid respiratory motion artifacts.

Fig. 1A–F This is the time-resolved CE-MRA of a 20-month-old boy with Kawasaki disease, showing bilateral small aneurysms of the proximal brachial artery. **A–F** Full-volume MIP images (after subtraction) of six consecutive dynamics (second to seventh dynamic) with a temporal resolution of 3.9 s per dynamic. The fourth dynamic (**C**) yielded the best arterial phase contrast and was chosen for further postprocessing. The manual injection of 0.2 mmol/kg of gadolinium contrast agent was made through an IV in the right foot. Imaging parameters were as follows: TR = 3.8 ms, TE = 1.2 ms, flip angle = 35°, matrix = 192×512 (reconstructed), 25 partitions 2.6 mm thick (reconstructed to 50 partitions of 1.3 mm thick), FOV = 440 mm with 70% reduced FOV, SENSE reduction factor of 4 (2 in the in-plane phase-encoding direction, 2 in the z direction), total of ten dynamics, total scan time of 39 s. A standard four-element body phased-array coil was used

Challenges in the pediatric population

As shown by a review of the literature, various groups have reported different methods to apply CE-MRA in children for a wide range of clinical applications [2–13]. There are many different approaches, partially because the pediatric population poses significant challenges to the standard techniques of CE-MRA. Infants and young children have a much higher heart rate with more rapid circulation times than adults and the

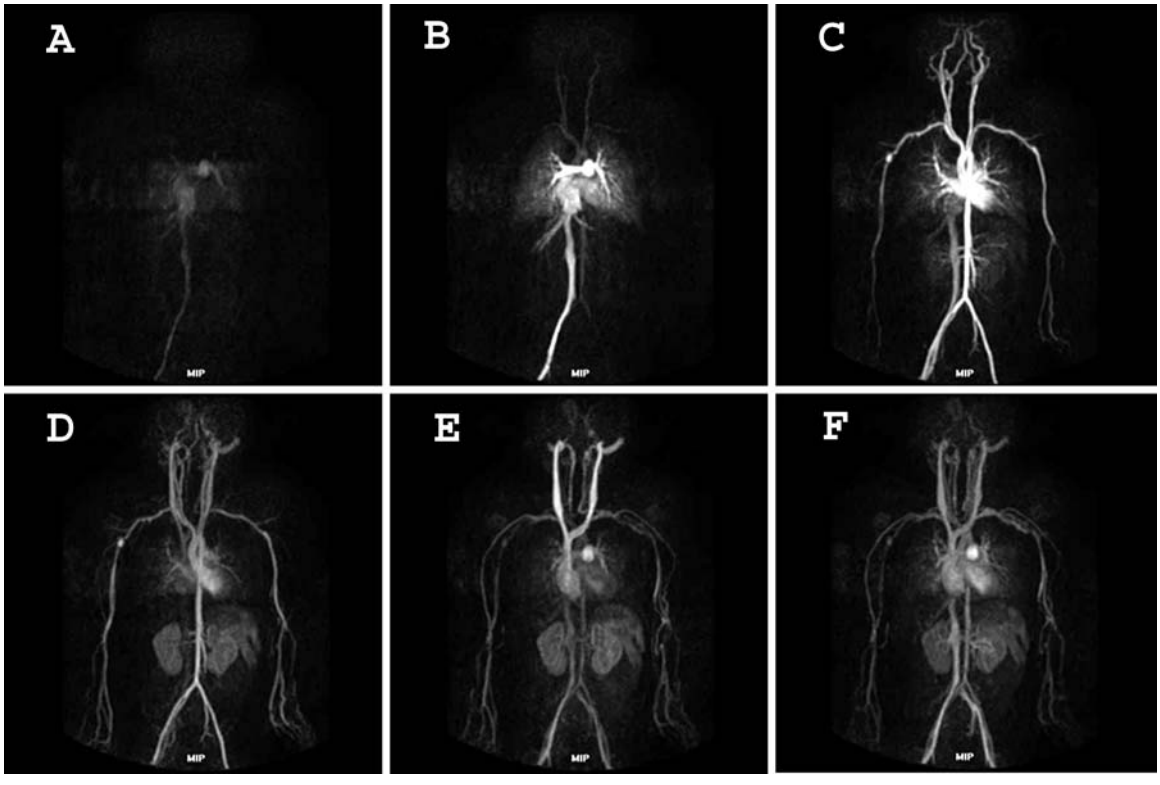

volume of contrast is much smaller. Double-dose contrast (0.2 mmol/kg) volume only amounts to a few milliliters. Therefore, the timing of the contrast bolus arrival is much more problematic. Breath-holding to minimize the respiratory motion artifacts is not possible in infants and children who are sedated for the MR examination rather than anesthesized and paralyzed. In the case of an unsedated child, the duration of breath-holding can be limited and unreliable. With these constraints, one approach that we have used is ''time-resolved'' CE-MRA [21, 22].

Table 1 Basic sequence: 3D T1-weighted fast gradient echo. Gadolinium contrast: 0.2 mmol/kg. Timing of injection of contrast: detailed in text

TR	Shortest
TE	Shortest
Flip angle	35°
FOV	Variable, depending on the size of patient[a]
Reduced FOV	60–70%[a]
Matrix	140–192 × 224–256 reconstructed to 256 × 512[b]
Thickness	2–3 mm on average; reconstructed to 1–1.5 mm[b]
Number of partitions	15–30 partitions[b]
SENSE reduction	2–4[b]
Scan time	3–6 s/dynamic[b]
Number of dynamics	As many as needed; average 7

[a]The combination of FOV and reduced FOV must include all the body parts along the in-plane phase-encoding direction of the 3D volume acquisition to avoid foldover artifact with SENSE [22]
[b]The combination of these parameters is adjusted to cover the anatomy of interest within 3–6 s. The younger the patient is, the shorter the scan time should be. A SENSE factor of 4 is achieved usually by a factor of 2 used along the in-plane phase-encoding direction and a factor of 2 in the z-direction of the 3D acquisition (along the direction of the partitions). This requires acquisition of a thicker volume of data in the z-direction. See Fig. 1 and legend

Fig. 2 Selected postprocessed images from a time-resolved CE-MRA performed on a 9-month-old infant, demonstrating the unusual anatomy of a persistent fifth arch. The infant was sedated and freely breathing at the time of the CE-MRA. **A** Full-volume MIP image after subtraction. **B–D** Thin-volume (1 mm thick) multiplanar reformated (MPR) images from the 3D data set, showing the origins of the four great vessels arising from the superior and smaller arch, with the persistent fifth arch being the larger and inferior arch (*arrow*) seen in continuity with the superior arch

A time-resolved CE-MRA technique and clinical examples

Short TR (< 5–6 ms) and short TE (< 2–3 ms) are now achievable by many MR scanners. Combined with a parallel imaging technique such as SENSE (SENSitivity Encoding) [19], the acquisition duration can be further shortened [21, 22]. Scan times of less than 5–6 s can be achievable without significant compromise of spatial resolution. All the clinical cases illustrated were acquired on either a 1.5 T Intera or NT-Intera at Release 8 level of software and hardware (Philips Medical Systems, Best, The Netherlands).

Practically speaking, the time-resolved CE-MRA is simply made up of multiple 3-D volumes (dynamics) acquired consecutively in the following fashion. The first dynamic is acquired prior to contrast injection to be used as the mask for subtraction in post-processing. Then, the subsequent dynamics are acquired consecutively without delay between each dynamic. There is no need to time the contrast injection, as it is started simultaneously with the start of acquisition of the subsequent dynamics. The total scan time depends on the number of dynamics used. Typically, seven dynamics are used and therefore the total scan time is approximately 30–45 s, depending on the acquisition time of each dynamic. The dynamics that depict the best arterial, or venous, or mixed arterial-venous phases will later be chosen for post-processing (Fig. 1). Typically, the source images are reviewed and multiplanar reformations

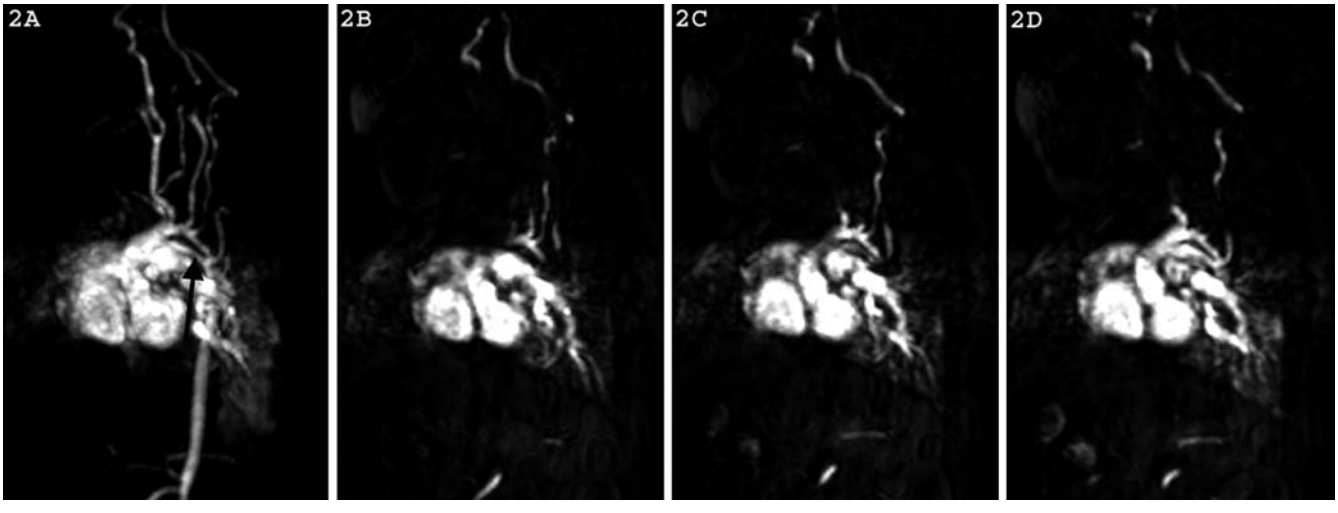

(MPR) are performed as needed for the diagnostic interpretation. In addition, the precontrast dynamic (the first dynamic) is used as the mask for subtraction, and maximum intensity projection (MIP) and 3D volume rendering are performed to display the vascular anatomy for the referring physicians. The pulse sequence parameters are shown in Table 1.

Based on our experience over the past 3 years, this time-resolved CE-MRA is easy to implement, eliminating the need for bolus timing. This is especially true in younger patients who cannot hold their breath reliably or sedated patients who really do not require general anesthesia, and thus respiration will not be suspended (Fig. 2). In addition, we found that CE-MRA is an extremely efficient sequence in terms of the amount of anatomic coverage per unit of scan time compared to other sequences (Fig. 3).

As the scan time for each dynamic shortens, the ability to separate the arterial and venous phases or pulmonary and systemic arterial phases increases (Fig. 4). We have also adapted this time-resolved CE-MRA technique in adolescent patients who can hold their breath. Depending on the ability of the patients to hold their breath and the duration of the 3D acquisition, 2–4 acquisitions can be made in one breath-hold (Figs. 4, 5, 6). In this situation, we time the arrival of contrast either by best estimate or by a real-time bolus

Fig. 3A–G Selected postprocessed images from a time-resolved CE-MRA performed on a newborn infant with heterotaxy. This infant was under general anesthesia for the MR examination because of his general medical condition, and the CE-MRA was performed with respiration suspended. By analyzing the source images, nearly all the extracardiac vascular anomalies in this infant with heterotaxy (asplenia) can be detected. **A–G** Selected coronal sections from a mixed arterial and venous dynamic from the CE-MRA arranged from posterior to anterior. Scan time for each dynamic was 6 s. **A** A left-sided descending aorta (*A*); **B**, **C** the total anomalous pulmonary venous return (TAPVR) below the diaphragm (*) and a left-sided IVC (*black arrows*) traversing through a transverse liver (*L*); **D** A right-sided stomach (*S*) with the transverse liver (*L*) and the TAPVR entering into a branch of the portal venous system (*black arrow*); **E** The confluence of hepatic veins entering into the left side of the floor of the atrium (*black arrow*); **E**, **F** show a right-sided SVC (*C*) with a patent left innominate vein (*I*) and a right-sided ascending aorta (*A*); **G** main portal vein (*PV*) spanning the transverse liver

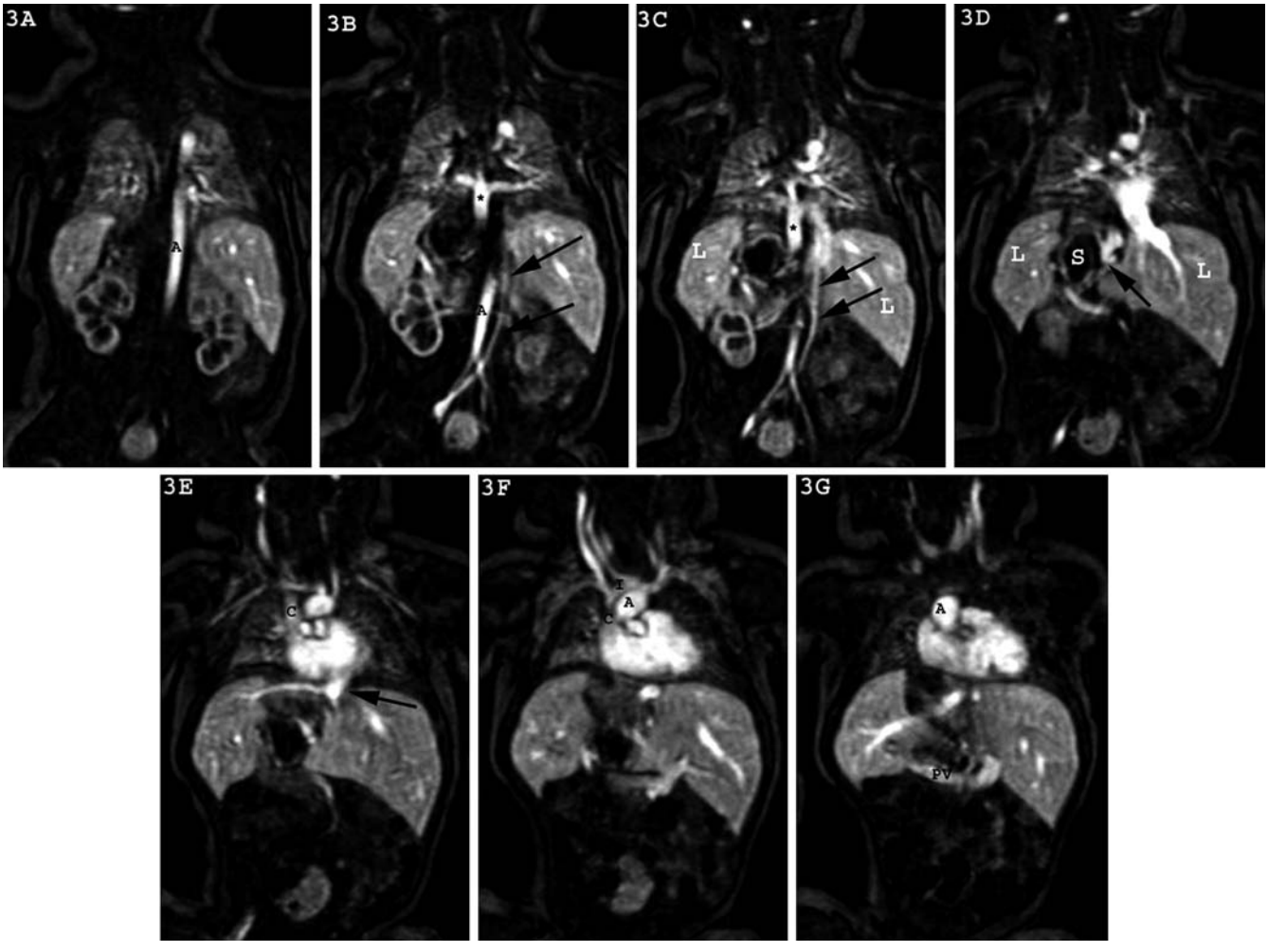

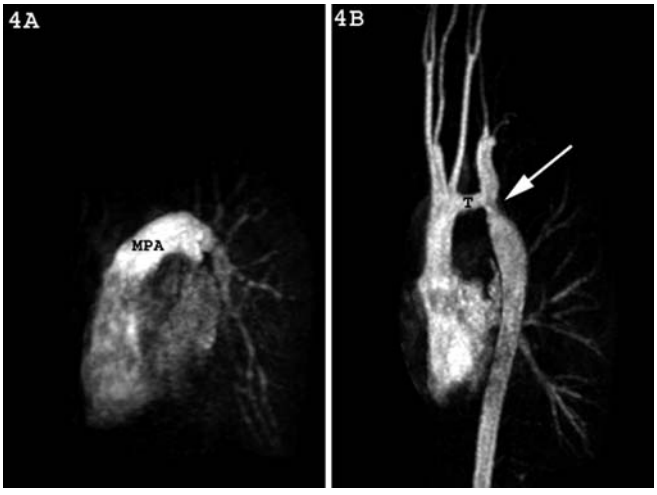

Fig. 4 This is an example of a cooperative 13-year-old boy with coarctation with poststenotic dilation. By using time-resolved CE-MRA with a temporal resolution of 2.5 s, the pulmonary and systemic arterial phases can be separated. Imaging parameters were as follows: TR = 4.2 ms, TE = 1.4 ms, flip angle = 35°, matrix = 154 × 512 (reconstructed), 15 partitions of 3.2 mm thick (reconstructed to 30 partitions of 1.6 mm thick), FOV = 400 mm with 60% reduced FOV, SENSE reduction factor of 3; a total of 11 dynamics, total scan time of 27.5 s. A standard four-element body phased-array coil was used. After the first dynamic acquired prior to contrast injection, 0.2 mmol/kg of Gadolinium contrast agent was injected at 2 mL/s, and patient was asked to hold his breath twice for approximately 12 s each time, starting at 8 s after initiation of contrast injection. **A**, **B** Full-volume MIP images of pulmonary arterial phase contrast and systemic arterial phase contrast, respectively. (*MPA* main pulmonary artery, *T* hypoplastic transverse arch, *arrow* discrete coarctation site)

tracking tool. Since the data acquisition duration is short, the timing of the arrival of contrast becomes less critical, and we tend to estimate when to start the scan after contrast injection, especially if the clinical situation does not mandate pure arterial phase imaging. When a bolus-tracking technique is used, it is important to know the time delay of switching from the bolus-tracking scan to the MRA scan, as the circulation in a pediatric patient is very rapid. A few seconds delay can cause the entire bolus to be missed completely. In our scanner, there is an approximately 3-s delay switching from the bolus-tracking sequence to the MRA sequence.

This technique can also be easily applied to the extremities. For example, in the evaluation of soft-tissue masses, postcontrast anatomic imaging is often performed. A CE-MRA can be obtained just prior to the post–contrast anatomic imaging, thus making use of the contrast that would have been given anyways. This can be achieved without significant prolongation of the total examination time since the time-resolved CE-MRA sequence is so easily implemented.

Additional vascular anatomic information and qualitative perfusion information of the soft-tissue mass can be obtained (Fig. 7).

Discussion

As illustrated by the clinical examples, CE-MRA can be applied to the chest, abdomen, and extremities. In our clinical experience, by far most of the clinical demand is for noninvasive evaluation of the great vessels in the chest. This is mainly in patients with congenital heart disease in whom echocardiography failed to depict the extracardiac vascular anatomy such as the aortic arch and descending aorta, pulmonary arteries, and pulmonary veins. This is especially so in postoperative patients where the acoustic window of transthoracic echocardiography may be poor. As multidetector row CT is becoming widely available, the choice between MRA and CTA will likely be determined by the local referral pattern, local expertise in the modalities, and availability of the scanners. CT is undoubtedly more easily available and a less complicated examination to perform, although the time-resolved MRA technique described here can also be easily applied. However, MR does not require ionizing radiation or an iodinated intravenous contrast agent. If the particular patient also requires the evaluation of ventricular function or intracardiac morphology, then MR is clearly the modality of choice.

It is important to point out that the described technique is only one of many methods now available to achieve time-resolved CE-MRA. Depending on the type of scanner hardware and software, a certain level of trade-off between spatial and temporal resolution can be determined at each individual site, depending on the clinical need, and, based on this, the scan parameters can be set. Recently, by reducing the scan time even further with strong and fast gradients achieving TR < 2 ms and TE < 1 ms, Balci et al. [23] used a 2-s-CE-MRA to separate pulmonary arterial and pulmonary venous phases in pediatric patients. Similarly, Finn et al. [24] also recently reported their initial experience in adult thoracic angiography using a subsecond MRA technique by compromising on the spatial resolution in the z-encoding direction (i.e., thicker partitions and therefore fewer partitions in the 3-D volume).

No matter which technique is used, or how rapid the acquisition can be, the quality of the CE-MRA will be higher with breath-holding. If the clinical question to be answered is whether there is a stenosis in a small vessel, then breath-holding is needed to maximize quality. Even then, the spatial resolution may not be adequate for certain clinical situations such as detection of branch renal artery stenosis (Fig. 6). However, in many clinical pediatric applications, the question is often one of

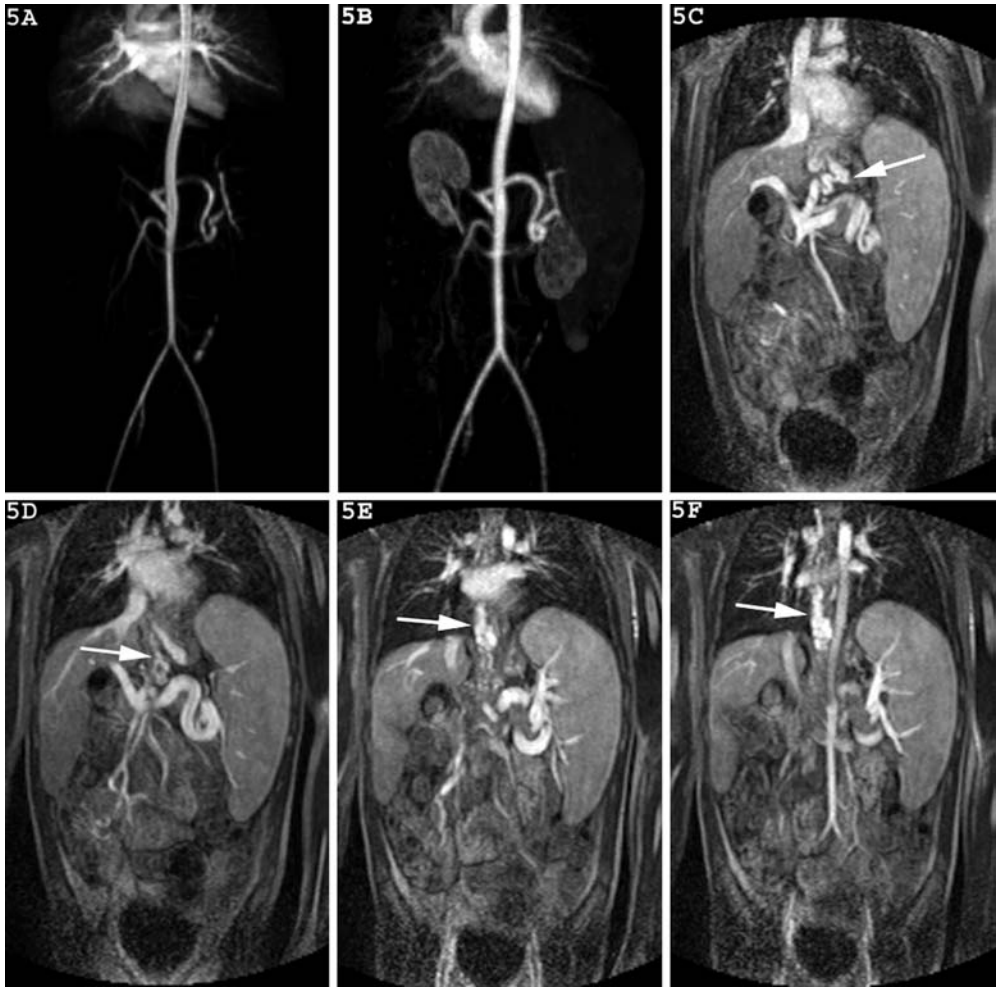

Fig. 5A–F This is a 12-year-old boy with short-gut syndrome and cirrhosis. He was well enough to perform 12-s breath-hold periods reliably. With the temporal resolution of the time-resolved CE-MRA at 6 s per dynamic, with a best-guess method to estimate the arrival of contrast to the abdominal aorta, we were able to obtain two consecutive dynamics with predominantly arterial phase contrast. **A**, **B** Postsubtraction, full-volume MIP images of consecutive dynamics. This is an example of the shorter scan duration per dynamic, providing a better chance of capturing arterial phase contrast. During the subsequent 12-s breath-hold, the portal venous phase was captured. **C**–**F** Selected thin-volume coronal MIP images from posterior to anterior, demonstrating the portal venous anatomy and the presence of significant varices (*arrows*). Also, note significant splenomegaly

anatomic location or connections or the presence or absence of certain vessels. A strong argument can be made that diagnostic quality CE-MRA can be achieved without the need for breath-holding.

Even accelerated by various schemes of rapid k-space trajectories and parallel imaging, the various techniques of CE-MRA are still restricted by a trade-off between temporal and spatial resolution. In order to achieve both high temporal and spatial resolution or to be able to capture first-pass arterial phase contrast with high spatial resolution on freely breathing pediatric patients, one may need to investigate the possibility of applying newer, different techniques. The kt-BLAST technique introduced by Tsao et al. [25, 26] seems to allow for high temporal and spatial resolution in real-time imaging of cardiovascular structures. This represents one potential solution by investigating the use of ultrafast imaging schemes on freely breathing pediatric patients. On the other end of the spectrum of speed of acquisition, Spuentrup et al. [27] reported on the combination of using respiratory navigator and arterial spin labeling to achieve high spatial-resolution 3D MR renal arteriogram on adults who were freely breathing. By allowing ample time for data acquisition that is synchronized to respiratory and cardiovascular physiologic motion, high spatial resolution is achieved, but with the penalty of long scan duration. Nonetheless, this also represents another potential solution to the problem of achieving high-resolution MRA in freely breathing pediatric patients.

Thus, with the rapid advances of MR techniques, it behoves the pediatric radiologist must take advantage of new and emerging techniques. With some modifications of these techniques, perhaps there will be a day when high temporal and spatial-resolution MRA or real-time MRA can be readily available for routine clinical use in the noninvasive evaluation of vascular anatomy in pediatric patients.

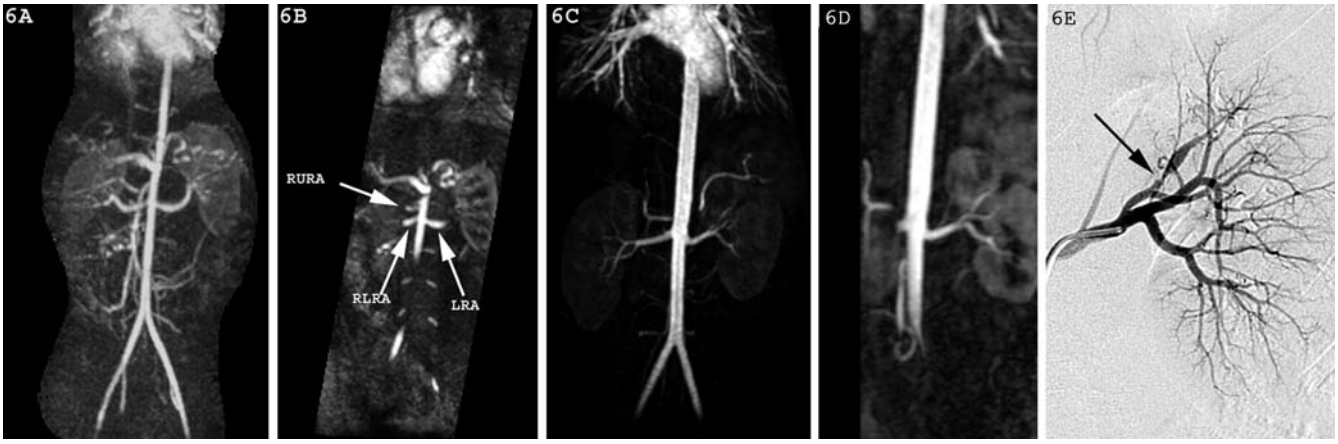

Fig. 6A–E Two examples of renal MRA by a time-resolved CE-MRA technique. **A** Full-volume MIP image after subtraction and **B** is a thin-volume MIP image in oblique coronal planes from a CE-MRA of a 13-year-old boy with Williams syndrome and hypertension. Two right renal arteries (*RURA* right upper renal artery, *RLRA* right lower renal artery) and a single left renal artery (LRA) all showed proximal stenoses. In addition, the entire abdominal aorta is diffusely narrowed. These findings were confirmed at conventional digital subtraction angiography (not shown). This CE-MRA was performed with the patient nonsedated and quietly breathing. Temporal resolution of the CE-MRA was 5 s per dynamic. **C** Full-volume MIP image after subtraction and **D** is a selected thin-volume MIP image in oblique coronal plane from the CE-MRA of a cooperative 11-year-old boy with hypertension who was able to hold his breath voluntarily for the time-resolved CE-MRA. With a SENSE factor of 3, a temporal resolution of 3.8 per dynamic was achieved with a true spatial resolution of $1.5 \times 1.8 \times 3.0$ mm reconstructed to $0.8 \times 1.0 \times 1.5$ mm. The left branch renal artery stenosis was difficult to detect, especially when compared with the invasive digital subtraction angiography with selective injection, **E** clearly demonstrating left branch renal artery stenosis (*arrow*). This example illustrates the difficulty in diagnosing branch renal artery stenosis by CE-MRA

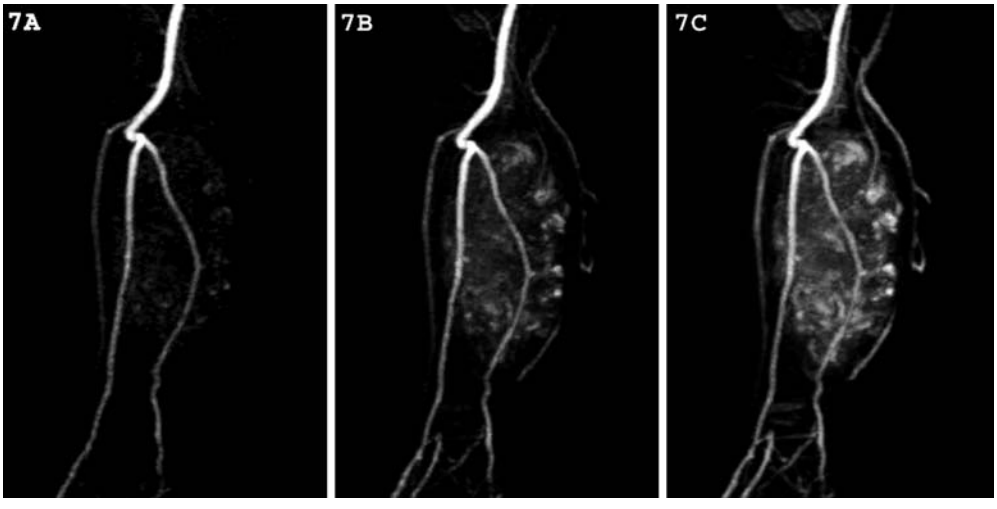

Fig. 7 This is a 2-year-old boy with a rhadomyosarcoma of the lower leg. **A**–**C** Full-volume MIP images after subtraction of consecutive dynamics from the time-resolved CE-MRA with a temporal resolution of 5 s/dynamic. The displacement of the major arteries in the lower leg by the tumor mass is clearly depicted. The rapid enhancement and tumor vascularity of the mass can also be appreciated

References

1. Prince MR, Yucel E, Kaufman J, et al (1993) Dynamic gadolinium-enhanced three-dimensional abdominal MR arteriography. J Magn Reson Imaging 3:877–881
2. Lam WW, Chan JH, Hui Y, et al (1998) Technical innovation: non-breath-hold gadolinium-enhanced MR angiography of the thoracoabdominal aorta: experience in 18 children. AJR 170:478–480
3. Haliloglu M, Hoffer FA, Gronemeyer SA, et al (1999) Applications of 3D contrast enhanced MR angiography in paediatric oncology. Pediatr Radiol 29:863–868
4. Pawlik HN, Chung T (1999) Initial clinical experience with non-breath-hold gadolinium-enhanced 3D-MR angiography of thorax and abdomen in infants and children with pathology. Proc Int Soc Magn Reson Med 7:1221
5. Teo EH, Strouse PJ, Prince MR (1999) Applications of magnetic resonance imaging and magnetic resonance angiography to evaluate the hepatic vasculature in the pediatric patient. Pediatr Radiol 29:238–243
6. Haliloglu M, Hoffer FA, Gronemeyer SA, et al (2000) 3D gadolinium-enhanced MRA: evaluation of hepatic vasculature in children with hepatoblastoma. J Magn Reson Imaging 11:65–68
7. Ng KK, Cheng YF, Wong KW, et al (2000) Gadolinium-enhanced magnetic resonance portography: application in paediatric liver transplant recipients. Transplant Proc 21:2099–2100
8. Holmqvist C, Larrsson E-M, Stehlberg F, et al (2001) Contrast-enhanced thoracic 3D-MR angiography in infants and children. Acta Radiol 42:50–58
9. Kondo C, Takada K, Yokoyama U, et al (2001) Comparison of three-dimensional contrast-enhanced magnetic resonance angiography and axial radiographic angiography for diagnosing congenital stenoses in small pulmonary arteries. Am J Cardiol 87:420–424
10. Kuroiwa M, Suzuki N, Hatakeyama S, et al (2001) Magnetic resonance angiogrpahy of portal collateral pathways after hepatic portoenterostomy in biliary atresia: comparisons with endoscopic findings, J Pediatr Surg 36:1012–1016
11. Hernandez RJ, Strouse PJ, Londy FJ, et al (2001) Gadolinium-enhanced MR angiography (Gd-MRA) of thoracic vasculature in an animal model using double-dose gadolinium and quiet breathing. Pediatr Radiol 31:589–593
12. Hernandez RJ (2002) Magnetic resonance imaging of mediastinal vessels. Magn Reson Imaging Clin N Am 10:237–251
13. Geva T, Greil GF, Marshall AC, et al (2002) Gadolinium-enhanced 3-dimensional magnetic resonance angiography of pulmonary blood supply in pateints with complex pulmonary stenosis or atresia: comparison with x-ray angiography. Circulation 106:473–478
14. Wilman AH, Riederer SJ (1997) Performance of elliptical centric view order for signal enhancement and motion artifact suppression in breath-hold three dimensional gradient echo imaging. Magn Reson Med 38:793–802
15. Wilman AH, Reiderer SJ, Houston J, et al (1998) Arterial phase carotid and vertebral artery imaging in 3D contrast-enhanced MR angiography by combining fluoroscopic triggering with an elliptical centric acquisition order. Magn Reson Med 40:24–35
16. Willinek WA, Gieseke J, Conrad R, et al (2002) Randomly segmented central k-space ordering in high-spatial-resolution contrast-enhanced MR angiography of the supraaortic arteries: initial experience. Radiology 225:583–585
17. Swan JS, Carroll TJ, Kennell TW, et al (2002) Time-resolved three-dimensional contrast-enhanced MR angiography of the peripheral vessels. Radiology 225:43–52
18. Vigen KK, Peters DC, Grist TM, et al (2000) Undersampled projection-reconstruction imaging for time-resolved contrast-enhanced imaging. Magn Reson Med 43:170–176
19. Sodickson DK, Manning WJ (1997) Simultaneous acquisition of spatial harmonics (smash): fast imaging with radiofrequency coil arrays. Magn Reson Med 38:591–603
20. Pruessmann KP, Weiger M, Schiedegger MB, et al (1999) SENSE: sensitivity encoding for fast MRI. Magn Reson Med 42:952–962
21. van den Brink JS, Watanabe Y, Kuhl CK, et al (2003) Implications of SENSE MR in routine clinical practice. Eur J Radiol 46:3–27
22. Muthupillai R, Vick GW III, Flamm SD, et al (2003) Free breathing time resolved contrast enhanced MRA in pediatric patients with sensitivity encoding. J Magn Reson Imaging 17:559–564
23. Balci NC, Talcin Y, Polat B, et al (2002) In: Book of abstracts of the 88th Annual Scientific Session of the RSNA, p 529, abstract no.1153
24. Finn JP, Baskaran V, Carr JC, et al (2002) Thorax: low-dose contrast-enhanced three-dimensional MR angiography with subsecond temporal resolution-initial reseults. Radiology 224:896–904
25. Tsao J, Behnia B, Webb AG (2001) Unifying linear prior-infomation-driven method for accelerated image acquisition. Magn Reson Med 46:652–660
26. Tsao J, Kozerke S, Boesiger P, et al (2003) Eight-fold acceleration in real-time cardiac imaging using k-t BLAST and k-t SENSE with SSFP and segmented EPI. Proc Int Soc Mag Reson Med 11:209
27. Spuentrup E, Manning WJ, Bornert P, et al (2002) Renal arteries: navigator-gated balanced fast field-echo projection MR angiography with aortic spin labeling: initial experience. Radiology 225:589–596